Available online at www.sciencedirect.com
ScienceDirect
Scripta Materialia 62 (2010) 183–186
Scripta MATERIALIA
www.elsevier.com/locate/scriptamat

Shear banding observations in Cu–16 wt.% Ag alloy subjected to one-pass equal channel angular pressing

Y.Z. Tian, W.Z. Han, H.J. Yang, S.X. Li, S.D. Wu and Z.F. Zhang*

Shenyang National Laboratory for Materials Science, Institute of Metal Research, Chinese Academy of Sciences, 72 Wenhua Road, Shenyang 110016, People's Republic of China

Received 15 September 2009; revised 13 October 2009; accepted 15 October 2009
Available online 20 October 2009

A coarse-grained Cu–16 wt.% Ag alloy was processed by equal channel angular pressing (ECAP) for one pass to reveal the shear deformation behaviors by scanning electron microscope and electron backscattering diffraction. The evolution of shear bands was found to be affected by both the parallel and vertical shearing to the intersection plane (IP) of the ECAP die, indicating that, besides the shearing along IP, the shearing vertical to it also plays an important role during the plastic deformation.

Keywords: Cu–Ag alloy; Equal channel angular pressing (ECAP); Shear bands

Severe plastic deformation (SPD) has attracted worldwide attention in recent years owing to its capability to substantially refine coarse-grained metals or alloys down to the sub-micrometer or nanometer level [1,2]. Several SPD techniques, such as equal channel angular pressing (ECAP) [3–8], high-pressure torsion [9], dynamic plastic deformation [10,11] and accumulative roll bonding [12], have been widely developed to produce ultrafine-grained (UFG) or nanocrystalline materials. Of these various techniques, ECAP is a promising process because it can produce bulk, fully dense and contamination-free UFG materials. It is generally accepted that the nature of the imposed deformation is simple shear along the intersection plane (IP) between the entrance and exit channels [8,13]. Recently, it has been suggested that, besides IP, a secondary shear plane (SSP) that is along the normal direction of IP also plays a role in shear deformation during ECAP [14–18]. Segal [8] has pointed out that there are two maximum shear stresses during ECAP. One is along IP and the other is vertical to it, providing the necessary conditions for shear deformations along two different shear planes. Han et al. [14–17] found that, besides the intense shear deformation along IP, the shear deformation along SSP also plays an important role in the plastic deformation; for example, they employed Cu and Al single crystals and bicrystals to successfully expound the effects of orientations and grain boundaries by taking SSP into account [14–17]. In addition, Wang et al. [18] demonstrated that shearing occurred on two shear planes when modeling the local texture evolution of Al alloys during ECAP. In this study, we employed a coarse-grained Cu–16 wt.% Ag alloy to further investigate the shear deformation during ECAP. The main feature of this special designed experiment is twofold: firstly, the decorative eutectic in Cu–16 wt.% Ag alloy can be conveniently used to trace the shear banding development because both the eutectic and the matrix have good deformation compatibility [19]; secondly, the billet was not fully extruded out in order to show the evolution processes of shear deformation during ECAP.

The details of microstructures and plastic deformation behavior of the Cu–16 wt.% Ag alloy in the present study can be found elsewhere [19]. Billets 8 mm in diameter and 45 mm in length were cut and extruded in a right-angle ECAP die with an outer arc of curvature of ~35° for one pass. One of the important features in the Cu–Ag alloy is that it possesses superiority in identifying the mechanical response, e.g. slip banding and shear banding. Since large shear strain is imposed during ECAP, the shear bands may be easily distinguished by observing the deformation of the decorative eutectic component. In order to study the shear banding evolution, the Y plane (as defined in Ref. [20]) of the billet was observed using a scanning electron microscope (SEM; LEO SUPRA 35). Note that all the shear bands investigated here were observed in the central region of

* Corresponding author. Tel.: +86 24 23971043; e-mail: zhfzhang@imr.ac.cn

1359-6462/$ - see front matter © 2009 Published by Elsevier Ltd. on behalf of Acta Materialia Inc.
doi:10.1016/j.scriptamat.2009.10.020

the samples, and shear bands in the near-surface region of the workpiece were excluded in order to avoid the influence of the friction. Several slices were investigated by the electron backscattering diffraction (EBSD) technique on the LEO SUPRA 35 SEM and a step size of 100 nm was used. The detailed information on the sample preparation can be seen elsewhere [19].

Before investigating the shear banding behavior, it is of value to note that the as-cast Cu–Ag alloy has relatively low strain-hardening ability, which should result in a small corner gap [21]. Moreover, the bigger outer arc of curvature is also related to the smaller corner gap [22]. Actually, the geometry of the workpiece is nearly the same as that of the ECAP die, and it is more reasonable to use the parameters from the workpiece than the ECAP die [21].

Figure 1 shows the whole microstructural evolution of the half-extruded billet after ECAP. The corresponding extrusion direction (ED) and insert direction (ID) are marked in Figure 1a. It is clearly recognized that the whole billet can be divided into three regions, denoted as regions A, B and C, respectively. Region A is the part just above the boundary of the fan region, which consists of the undeformed equiaxed microstructure; the eutectic component begins to be elongated in the fan region (region B), separated by the plane OO_1, which is consistent with the previous results [23]; while in region C, the eutectic component can be seen to have been severely distorted. In region B, there are two kinds of shear bands along different directions with respect to ED, as shown in Figure 1b and c, and the corresponding sites are indicated by circles 1 and 2, respectively. Figure 1b shows that two shear bands pass through the eutectic component, leaving some deformation-induced steps, as indicated by the arrows. This is similar to the shear deformation near the grain boundary in Cu bicrystals extruded by ECAP for one pass [15].

In region C (see Fig. 1a), the two kinds of shear bands were found more frequently, as shown in Figure 1d and e. Figure 1d shows a shear band of about 5 μm in width, and there are some deformation-induced steps in the intersection of the eutectic and the shear band, as indicated by the arrows. The eutectic component was found to have severely sheared and thinned inside the shear band. Moreover, the precipitates were also sheared, indicating that a large shear strain was extraordinarily imposed there. Figure 1e shows several shear bands with different shear directions.In order to identify the characteristics of the two kinds of shear bands further, the EBSD technique was used to reveal the shear banding behavior. The two kinds of shear bands in region C are exhibited in Figure 2a and b and Figure 2c and d, respectively. Figure 2a shows one kind of shear band ~4 μm in width, while the detailed information inside the broken rectangle is characterized by EBSD, as shown in Figure 2b. The high-angle boundaries (HABs, $\geqslant 15°$) are indicated by the black lines. The inset shows the {1 1 1} pole figure. It is found that the shear band and the matrix are separated by HABs. The {1 1 1} plane, as indicated by the broken line, is approximately parallel to the shear band, indicating that the banding structure propagated along the {1 1 1} plane. The other shear band shown in Figure 2c and d propagated along the {1 1 1} plane. It is worth noting that there are many shear bands with different shear angles in the same coarse grain, indicating that some of them may not propagate along the {1 1 1} plane.

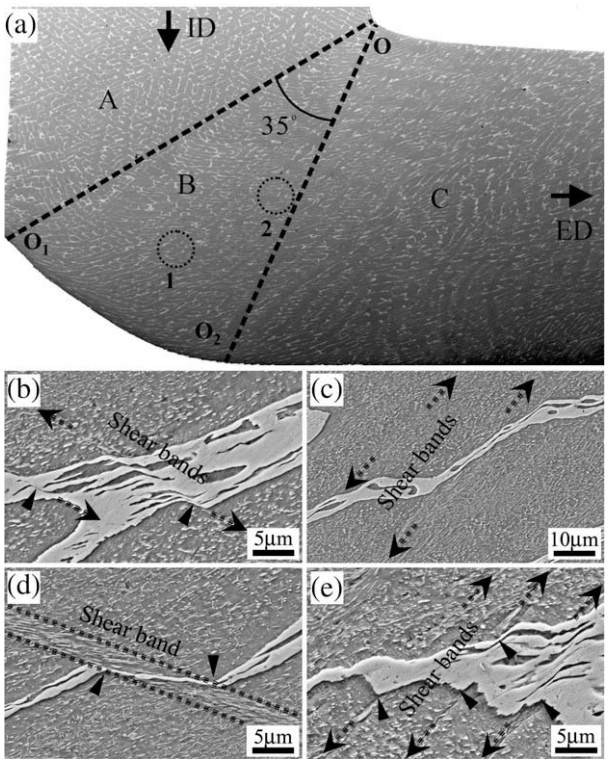

Figure 1. (a) Microstructural evolution of the half-extruded Cu–16 wt.% Ag alloy subjected to ECAP for one pass (Y plane); (b and c) shear banding observation in circles 1 and 2 in region B, respectively (see (a)); (d and e) shear banding observation in region C (see (a)).

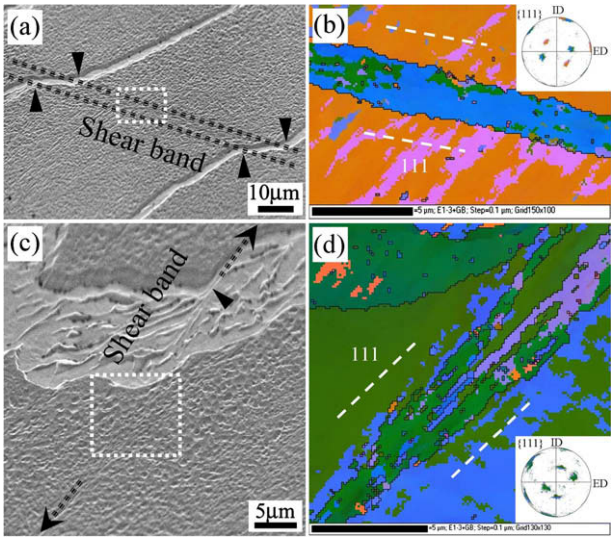

Figure 2. Shear banding observation in region C: (a and b) one kind of shear band and the corresponding EBSD map of the broken rectangular region; (c and d) the other kind of shear band and the corresponding EBSD map of the broken square region. The horizontal direction corresponds to ED.

We labeled the two kinds of shear bands depicted above as *SBI* and *SBII*, as shown in Figure 3b; the shear angles with respect to ED correspond to $\alpha 1$ and $\alpha 2$, respectively. The statistic values of the shear angles in regions B and C are shown in Figure 3a and b, respectively. It is generally recognized that high strain is imposed by simple shear along IP during ECAP [8,13]. Similarly, in this study, any plane ranging from OO_1 to OO_2 in the fan region is defined as IP for simplicity (see Fig. 4a). In that case, when shear deformation occurred along IP at any shear site θ, the shear angle should be $\alpha = \theta + 31°$, according to the geometrical parameters shown in Figure 4a. Note that θ falls in the range of $0° \leqslant \theta \leqslant 35°$ in region B (see Fig. 4a). Moreover, any shear band developed before θ should be approximately stable in the shear direction before crossing IP OO_2 (see Figure 4c), since the total moving distance at any point of the shear band must be identical [23]. For example, when shear deformation occurs along IP OO_1, the shear angle α should be equal to 31°, and this shear angle should not change greatly when it flows in the fan region. This means that the final shear angle α should be in the range of $31° \leqslant \alpha \leqslant \theta + 31°$ at any site θ in the fan region. Interestingly, most of the statistical values of the shear angles fall well within the calculated range, as shown in Figure 3a. However, many exceptional shear bands were also observed, indicating that other shearing mechanism may be involved. Considering the distribution of the shear bands in the fan region, more shear bands are found to exist near IP OO_2, indicating that a large shear strain may be imposed there.

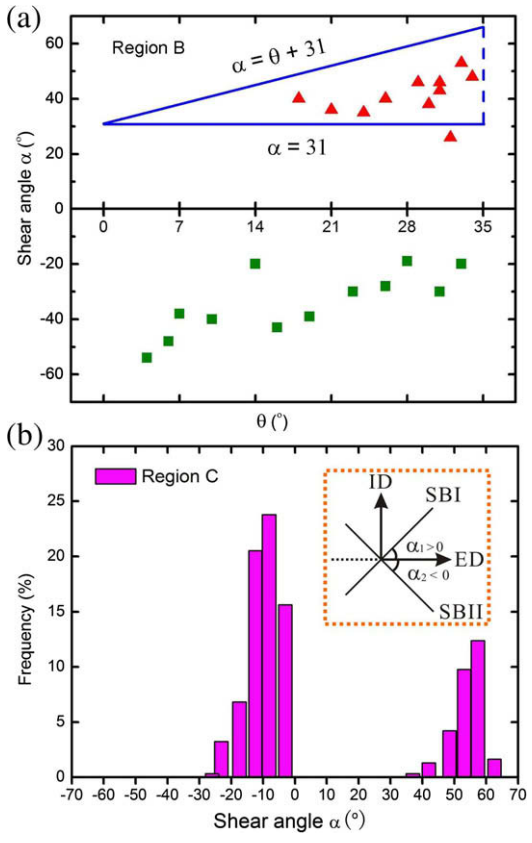

Figure 3. Distribution of the shear angles with respect to ED in (a) region B and (b) region C. θ is defined as the angle from the shear plane OO_1 in the fan region, as shown in Figure 4a.

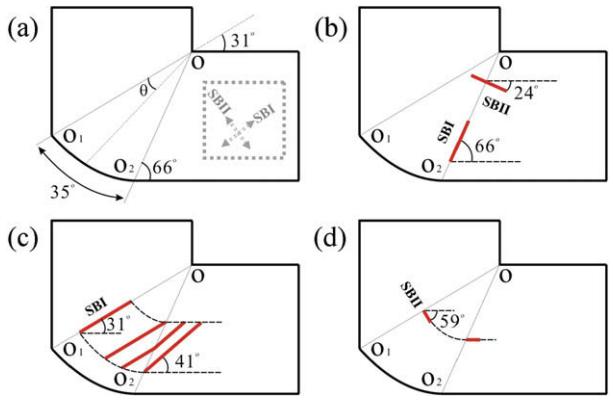

Figure 4. (a) Illustration of the geometrical parameters of the die; (b) illustration of the shear banding along and vertical to the plane OO_2; (c) formation and evolution of *SBI* along the plane OO_1; (d) formation and evolution of *SBII* along the plane OO_1. The horizontal direction corresponds to ED.

In region C, the experimental results show that the shear angles are in the ranges of $38° < \alpha_{1CE} < 64°$ and $-26° < \alpha_{2CE} < 0°$, respectively, as shown in Figure 3b. Considering the bilateral distribution of the shear bands, it is necessary to clarify how, besides the shear deformation along IP (*SBI*), the secondary shear banding (*SBII*) affects the shear deformation of the materials subjected to ECAP [14–18].

Based on the experimental results above, it is of value to discover the shear deformation mechanism of the Cu–Ag alloy during ECAP. The geometrical parameters of the die are illustrated in Figure 4a. Previously, Segal [8] pointed out that there are two maximum shear stress directions during ECAP: one along IP and the other one vertical to it. In the physical modeling experiment using millet grains, shear deformation was found to occur only in the deformation zone with a fan shape, and to start and end at the boundaries of the zone [23]. Based on the theoretical predictions and experimental results depicted above, it is proposed that there are two kinds of shear deformation that occur in the fan region, as illustrated in the inset in Figure 4a. The two marginal planes of the fan region, OO_1 and OO_2, are especially important because they determine the ranges of the shear angles. Supposing that the two shear deformations occur both along and vertical to IP OO_2, the theoretical shear angles should be 66° and −24°, respectively (see Fig. 4b), and will not change their directions after entering region C, which is out of the scope of the plastic deformation zone. In contrast, the shear deformations along and vertical to IP OO_1 should be very different, because they occur just before entering the fan region, and the shear bands will continuously rotate in the fan region due to metal flow [23]. Supposing *SBI* is along IP OO_1 (31° with respect to ED), based on the case that the total moving distance of any point must be identical within the same time [23], it will rotate to ~41° after leaving the fan region according to the flow line field analysis proposed by Han et al. [23,24], as shown in Figure 4c. On the other hand, *SBII* (vertical to IP OO_1), that is inclined to −59° with respect to ED, will

move along the outer arc of curvature, and then parallel to ED in the horizontal channel after leaving the fan region, evolving to approximately 0° according to the experiment using millet grains [23]. Based on the predictions elucidated above, it is easy to identify that the two kinds of shear angles should have theoretical ranges of $41° < \theta_{1CT} < 66°$ and $-24° < \theta_{2CT} < 0°$ in region C. It is clear that the experimental results (see Fig. 3b) fall well in the predicted ranges of shear angles.

In conclusion, the present results further substantiate the existence of the two shear deformations in ECAP: one is along IP, the other is vertical to it. The experimental results of the shear angles fall well within the predicted ranges that are analyzed based on the two kinds of shear deformations.

The authors are grateful to Mrs. W. Gao and Dr. H.F. Zou for the help with the SEM and EBSD observations. Dr. P. Zhang and Dr. X.H. An are also acknowledged for their help in conducting the ECAP experiments. This work was supported by National Natural Science Foundation of China (NSFC) under Grant No. 50890173 and the National Outstanding Young Scientist Foundation under Grant No. 50625103.

[1] M.A. Meyers, A. Mishra, D.J. Benson, Prog. Mater. Sci. 51 (2006) 427.
[2] Y.T. Zhu, T.C. Lowe, T.G. Langdon, Scr. Mater. 51 (2004) 825.
[3] R.Z. Valiev, T.G. Langdon, Prog. Mater. Sci. 51 (2006) 881.
[4] Y.H. Zhao, X.Z. Liao, Z. Jin, R.Z. Valiev, Y.T. Zhu, Acta Mater. 52 (2004) 4589.
[5] T.G. Langdon, M. Furukawa, M. Nemoto, Z. Horita, JOM 52 (2000) 30.
[6] A. Mishra, B.K. Kad, F. Gregori, M.A. Meyers, Acta Mater. 55 (2007) 13.
[7] F. Dalla Torre, R. Lapovok, J. Sandlin, P.F. Thomson, C.H.J. Davies, E.V. Pereloma, Acta Mater. 52 (2004) 4819.
[8] V.M. Segal, Mater. Sci. Eng. A 271 (1999) 322.
[9] A.P. Zhilyaev, T.G. Langdon, Prog. Mater. Sci. 53 (2008) 893.
[10] Y.S. Li, N.R. Tao, K. Lu, Acta Mater. 56 (2008) 230.
[11] N.R. Tao, K. Lu, J. Mater. Sci. Technol. 23 (2007) 771.
[12] Y. Saito, H. Utsunomiya, N. Tsuji, T. Sakai, Acta Mater. 47 (1999) 579.
[13] V.M. Segal, Mater. Sci. Eng. A 345 (2003) 36.
[14] W.Z. Han, Z.F. Zhang, S.D. Wu, S.X. Li, Acta Mater. 55 (2007) 5889.
[15] W.Z. Han, H.J. Yang, X.H. An, R.Q. Yang, S.X. Li, S.D. Wu, Z.F. Zhang, Acta Mater. 57 (2009) 1132.
[16] W.Z. Han, Z.F. Zhang, S.D. Wu, S.X. Li, Scr. Mater. 59 (2008) 421.
[17] W.Z. Han, Z.F. Zhang, S.D. Wu, S.X. Li, Philos. Mag. 88 (2008) 3011.
[18] S.C. Wang, M.J. Starink, N. Gao, X.G. Qiao, C. Xu, T.G. Langdon, Acta Mater. 56 (2008) 3800.
[19] Y.Z. Tian, Z.F. Zhang, Mater. Sci. Eng. A 508 (2009) 209.
[20] Y. Iwahashi, M. Furukawa, Z. Horita, M. Nemoto, T.G. Langdon, Metall. Mater. Trans. A 29 (1998) 2245.
[21] H.S. Kim, M.H. Seo, S.I. Hong, Mater. Sci. Eng. A 291 (2000) 86.
[22] W. Wei, A.V. Nagasekhar, G. Chen, Y. Tick-Hon, K.X. Wei, Scr. Mater. 54 (2006) 1865.
[23] W.Z. Han, Z.F. Zhang, S.D. Wu, S.X. Li, Mater. Sci. Eng. A 476 (2008) 224.
[24] W.Z. Han, Z.F. Zhang, S.D. Wu, S.X. Li, Philos. Mag. Lett. 87 (2007) 735.